

## Characterization and Electrocatalytic Properties of the Phosphomolybdate-PAMAM Nanocomposite Film

Daolin Zhu<sup>1</sup>, and Shouguo Wu<sup>2</sup>, Yijiang Shao<sup>1,\*</sup>

<sup>1</sup> Department of Biotechnology, Hefei Technology College, Chaohu 238000, P. R. China

<sup>2</sup> Department of chemistry, University of Science and Technology of China, Hefei, Anhui, 230026, P.R. China

\*E-mail: [shaoyijiang@126.com](mailto:shaoyijiang@126.com)

Received: 28 February 2019/ Accepted: 2 August 2019 / Published: 30 August 2019

---

The phosphomolybdate-PAMAM nanocomposite film was successfully prepared by using a submonolayer of 3-mercaptopropionic acid (3-MPA) adsorbed on a polycrystalline gold electrode further reacted with poly(amidoamine) (PAMAM) dendrimer (generation 4.0) to obtain a film on which 1:12 phosphomolybdate acid (PMO<sub>12</sub>) was later coordinated to afford a mixed electrocatalytic layer. On the basis of the electrochemical behaviors, atomic force microscopy (AFM) and X-ray photoelectron spectra (XPS), it is suggested that the PMO<sub>12</sub> nanoparticles are located within the dendritic structure of the surface attached PAMAM dendrimers. The protonated environment provided by PAMAM not only promises the higher electroactivity of PMO<sub>12</sub> at weak acidic condition, but also improves its stability. It was illustrated experimentally that the hybrid film showed a high electrocatalytic activity for reduction of S<sub>2</sub>O<sub>8</sub><sup>2-</sup> and H<sub>2</sub>O<sub>2</sub> in the aqueous solution of pH 4.0.

---

**Keywords:** Phosphomolybdate acid (PMO<sub>12</sub>), PAMAM, Nanocomposite, Electrocatalysis, S<sub>2</sub>O<sub>8</sub><sup>2-</sup>, H<sub>2</sub>O<sub>2</sub>.

### 1. INTRODUCTION

Isopolyoxometallates and heteropolyoxometallates are polynuclear complexes of Mo(VI), W(VI) and V(V) which can also involve other elements as central atoms or ligands [1]. Phosphomolybdate acid (PMO<sub>12</sub>) is one of the most important isopolyoxometallates. It is a highly efficient catalyst, and possesses fast reversible multi-electron redox characteristics under moderate conditions. Phosphomolybdate acid can accept and release a certain number of electrons without decomposition, thus serving as multielectron relays. It is a multi-electron oxidant and, at the same time, is a strong Bronsted acid. It can be used as both homogeneous and heterogeneous oxidation and acid catalyst, as well as bifunctional catalyst. Therefore, phosphomolybdates have been widely used in organic synthesis [2,3], oxidation of organic compounds [4-6], corrosion protection [7-9,8,3], supercapacitor [10-12,9,1.2], non-carbon full cells [13-18,10-15], and chemically modified electrodes for analytical applications [19-25,16-22].

Especially, in the recent years, phosphomolybdates have been more and more used as electrocatalysts [26-34,4,5,23-29]. Nunes et al [28] used phosphomolybdate@carbon-basednanocomposites as electrocatalysts for oxygen reduction reaction. Fernandes and coworkers [29] used the carbonnanomaterial-phosphomolybdatecomposites for oxidative electrocatalysis. Ding et al [22] immobilized the  $\text{PMo}_{12}$ @poly(diallyldimethylammonium chloride)-reduced graphene oxide on the glass carbon electrode for highly efficient electrocatalytic reduction of bromated. Wang and coworkers [30] investigated the electrochemical oxidation of Acid Red 3R with the new catalyst of iron phosphomolybdate ( $\text{FePMo}_{12}$ ) supported on modified molecular sieves. Manivel et al [32] constructed a silver nanoparticles embedded phosphomolybdate-polyaniline hybrid electrode for electrocatalytic reduction of  $\text{H}_2\text{O}_2$ . Skunik et al [33] studied the phosphomolybdate-modified multi-walled carbon nanotubes for electrocatalytic reduction of bromated. Chen et al [34] investigated the electrocatalytic properties of composite poly(new fuchsin) and phosphomolybdate films. However, most of these works were carried out in strong acidic solutions. When the pH of solution is higher than two, the phosphomolybdates are unstable due to their redox reactions need participation of protons.

Dendrimers are a relatively new class of materials. Due to their intrinsic and exciting properties, there have been increasing interests in applying dendrimers to the related areas such as drug delivery, protein models, molecular antennas, and catalytic materials [35,36]. Dendrimers have also been used in chemically modified electrodes, some recent reports indicate that these materials are capable of increasing the concentration of hydrophobic molecules at the electrode-solution interface, so that improving the sensitivity as well as the selectivity of certain specific electrochemical reactions. Among various dendrimers, poly(amidoamine) (PAMAM) is the most frequently studied. Godinez modified gold bead electrode with PB containing starburst PAMAM dendrimer to afford mixed and stable electrocatalytic layers which not only showed an improved surface coverage of PB on the dendrimer modified electrode but also showed an enhanced stability at neutral pH values [37]. In the previous work, we have successfully developed a stable and selective sensor of hydrogen peroxide based on PB/PAMAM complex membrane [38]. Long et al fabricated HPA/PAMAM multilayer films by the LBL deposition of oppositely charged species based on electrostatic attraction [39, 40]. Herein, we prepared a simple  $\text{PMo}_{12}$ /PAMAM monolayer modified electrode, investigated its electrochemical behaviors in aqueous solutions of different pH, especially its electrocatalytic activity in weak acidic solutions, and evaluated the stability and catalysis of phosphomolybdate in weak acidic media.

## 2. EXPERIMENTAL

### 2.1 Materials and Equipment

PAMAM generation 4.0 dendrimer (bearing 64  $-\text{NH}_2$  terminal functional group) was obtained from Aldrich. 1-(3-(dimethylamino)propyl)-3-ethyl carbodiimide hydro-chloride (EDC) and  $\text{HS}(\text{CH}_2)_2\text{COOH}$  were obtained from A Johnson Matthey Company. HPLC grade methanol, acetone, sodiumphosphomolybdate (1:12),  $\text{H}_2\text{O}_2$  (30% w/v solution) and  $\text{K}_2\text{S}_2\text{O}_8$  were from Shanghai Chemical Reagents (Shanghai, China). All chemicals were of analytical grade and used without further purification.

Doubly distilled water was used for preparation of the working solutions. All experiments were carried out at room temperature.

The LK2006 electrochemical analysis system (LANLIKE, Tianjin, China) was employed for cyclic voltammetric and amperometric measurements. All measurements were carried out with a three-electrode cell comprising a  $\text{PMo}_{12}$ -PAMAM/3-MPA/Au electrode as a working electrode, a platinum wire counter electrode, and a saturated calomel reference electrode.

AFM measurements were performed using a Digital Nanoscope IIIa multimode system (DI, Santa Barbara, CA, USA). The XPS spectra were recorded on a VG ESCALAB MKIIX-ray photoelectron spectrometer, using non-monochromated Al  $K\alpha$  radiation as the excitation source.

## 2.2 Preparation of the $\text{PMo}_{12}$ -PAMAM/Au electrode

The bare polycrystalline gold electrode (4 mm diameter) was first polished with abrasive paper, and then with alumina (0.3  $\mu\text{m}$ ) and rinsed thoroughly with water. The polished gold electrode was immersed in Piranha solution for 20 min, followed by sonicating in acetone and distilled water for 5 min respectively to remove the surface organic and inorganic compounds of the electrode. After that the electrode was cycling scan in 0.5 mol  $\text{L}^{-1}$   $\text{H}_2\text{SO}_4$  solution with cyclic voltammetry until a stable cyclic voltammogram was obtained. The pretreated gold electrode was immersed in 1.0 mmol  $\text{L}^{-1}$  methanol solution of 3-MPA for 24 h at room temperature, and then washed thoroughly in an ultrasonic bath with distilled water to remove the non-chemisorbed materials. Subsequently, the 3-MPA/Au modified electrode was immersed in 21  $\mu\text{mol L}^{-1}$  methanol solution of PAMAM dendrimer in presence of 5.0 mmol  $\text{L}^{-1}$  EDC for 24 h at room temperature without stirring. Thus the PAMAM/3-MPA/Au self-assembled membrane (SAM) was obtained. The prepared PAMAM/3-MPA/Au electrode was then dipped in 0.5 M  $\text{H}_2\text{SO}_4$  solution containing 0.5 mM phosphomolybdate(1:12) for 12 h at room temperature. Finally the electrode was taken out and rinsed thoroughly with deionized water. The  $\text{PMo}_{12}$ -PAMAM/Au modified electrode was fabricated in this way.

## 3. RESULTS AND DISCUSSION

### 3.1 Physical characteristics of the $\text{PMo}_{12}$ -PAMAM/Au electrode

The surface AFM images of the modified electrodes are shown in Fig. 1. Fig. 1a depicts an image of 3-MPA film incorporated into a polycrystalline gold electrode surface. Although the fraction of the electrode surface chemically modified is far less than unity, the thiol molecules in this submonolayer are not forming islands or clusters but instead are individually distributed across the electrode surface [41]. Fig. 1b presents an image of PAMAM/3-MPA/Au. The features consistent with the dimensions of individual dendrimer molecules are not seen in this image, but instead larger patchy features are observed which probably attribute to the formation of peptide bond between 3-MPA and PAMAM. Fig. 1c takes on the nanolayer of the  $\text{PMo}_{12}$  anions. The diameter of the clusters is from several nanometers to about one hundred nanometers, which is larger than the diameter of the  $\text{PMo}_{12}^{3-}$  anion. This may be attributed to the formation of larger clusters of  $\text{PMo}_{12}^{3-}$  aggregates during the self-assembly process. It is interesting

to note that the  $\text{PMo}_{12}^{3-}$  clusters are individually distributed across the electrode surface, which obviously different from the conventionally self-assembly  $\text{PMo}_{12}$  clusters which connected to each other to form a network structure [42, 43]. The phenomenon reveals that the PAMAM dendrimers prevent  $\text{PMo}_{12}$  clusters from assembling, and suggests there is an interaction between the dendrimer molecule and the  $\text{PMo}_{12}$  species.

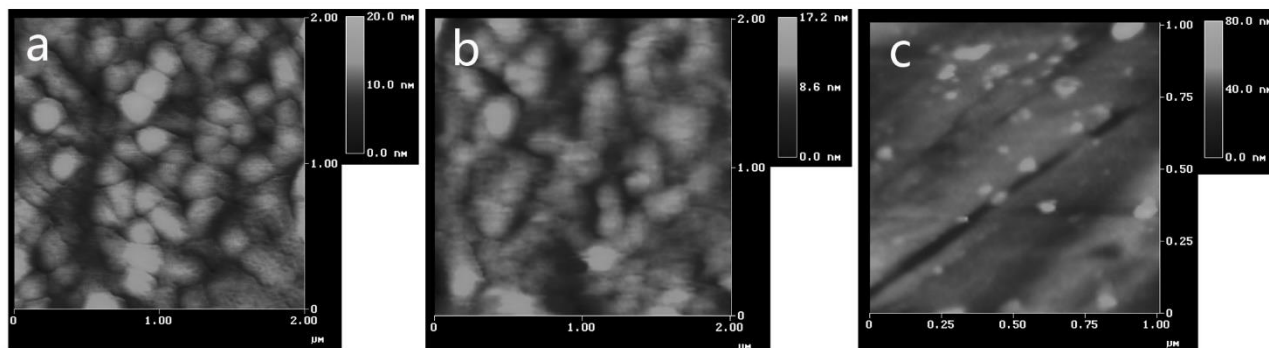


**Figure 1.** Representative topography images of the self-assembled membrane surfaces formed through deposition of (a) the 3-MPA (b) PAMAM/3-MPA, and (c)  $\text{PMo}_{12}$ /PAMAM/3-MPA onto the polycrystalline gold slice (images obtained in air).

The attachment of 3-MPA to the surface of the gold electrode has been proved by XPS data (see Fig. 2a). At the 3-MPA modified gold electrode, the characteristic peak of C 1s occurred at about 284.65 eV for C-C, 286.45 eV for C-S and 288.66 eV for COOH. As shown in Fig. 2b and 2c, the peak of C 1s for C-C, C-S and COO<sup>-</sup> are similar to Fig. 2a, but the typical peaks of C-N at about 286.24 eV prove the PAMAM dendrimer anchored on the surface of the electrode by bonding with 3-MPA, namely, the peptide bond was formed between the dendrimer and thiol molecule. We noted that there was no characteristic N 1s peak on 3-MPA modified electrode, but for PAMAM/3-MPA/Au electrode and  $\text{PMo}_{12}$ /PAMAM/3-MPA/Au electrode, N 1s peaks were observed in Fig. 2d at 400.27 eV resulting from the  $-\text{NH}_2$  group and 402.30 eV corresponding to amino carboxylic group. From Fig. 2e, it is clear that the Mo exists in the multilayer. The characteristic peaks of Mo 3d at 231.55 eV, 232.80 eV, 234.67 eV, 235.92 eV and Mo 3p at 395.79 eV and 398.09 eV respectively, prove that PAMAM dendrimer is capable of hosting  $\text{PMo}_{12}$  molecule.

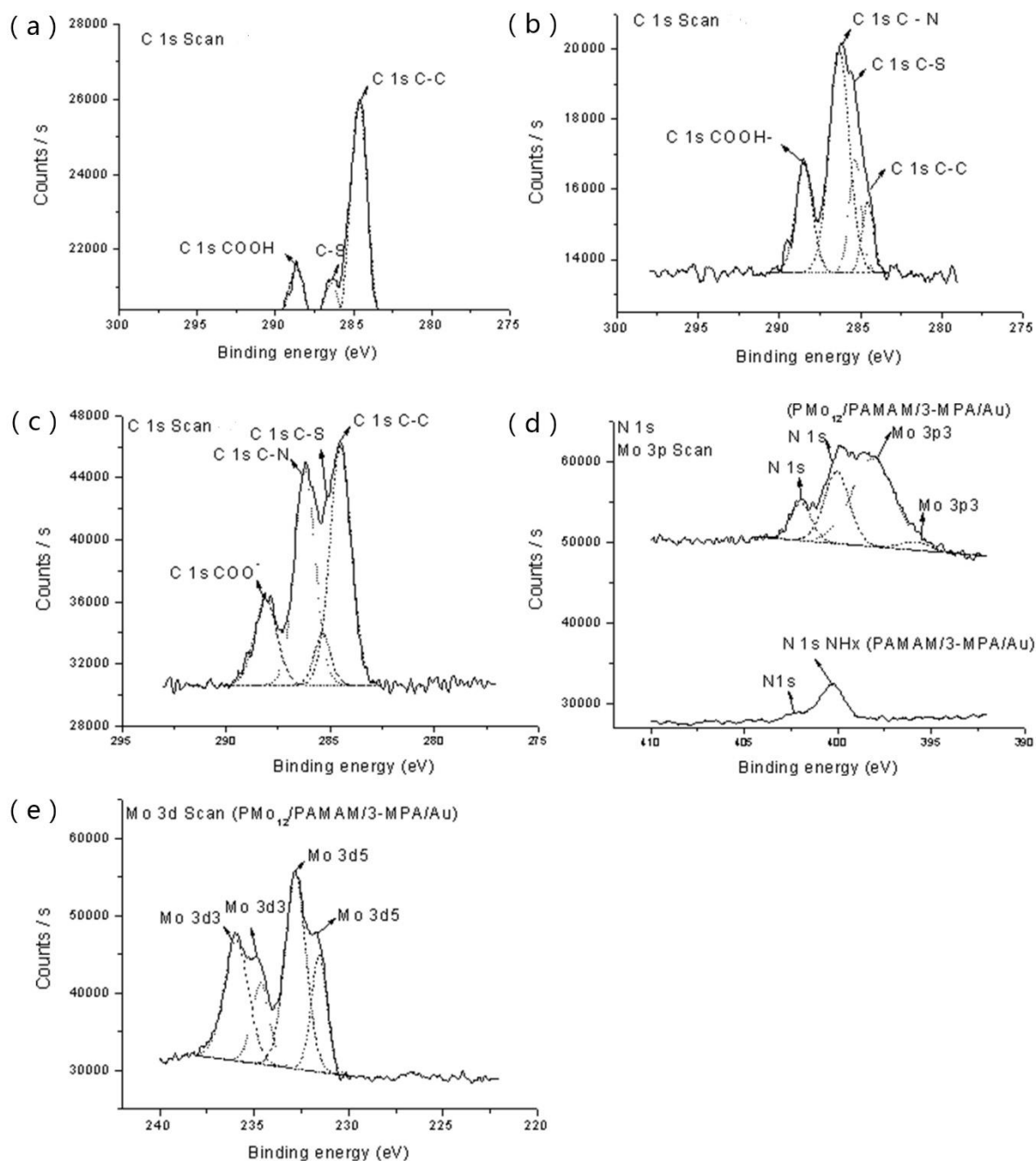


**Figure 2.** XPS detailed spectra of (a) the C 1s region for 3-MPA/Au, (b) the C 1s region for PAMAM/3-MPA/Au, (c) the C 1s region for the PMo<sub>12</sub>/PAMAM/3-MPA/Au, (d) the N 1s region for PAMAM/3-MPA/Au and PMo<sub>12</sub>/PAMAM/3-MPA/Au and the Mo 3p region for PMo<sub>12</sub>/PAMAM/3-MPA/Au and (e) the Mo 3d region for PMo<sub>12</sub>/PAMAM/3-MPA/Au.

### 3.2. Electrochemical behaviors of the PMo<sub>12</sub>-PAMAM/Au electrode

The electrochemical behaviors of the PMo<sub>12</sub>-PAMAM/Au electrode in different pH solutions are displayed in Fig. 3(A, B, C). For comparison, the cyclic voltammetry (CV) responses of PMo<sub>12</sub>/graphite electrode are also provided (D, E, F). The modified electrodes were taken out from the modified solution,

and rinsed with deionized water. The cyclic voltammograms of the modified electrodes were recorded in pure buffer solutions.

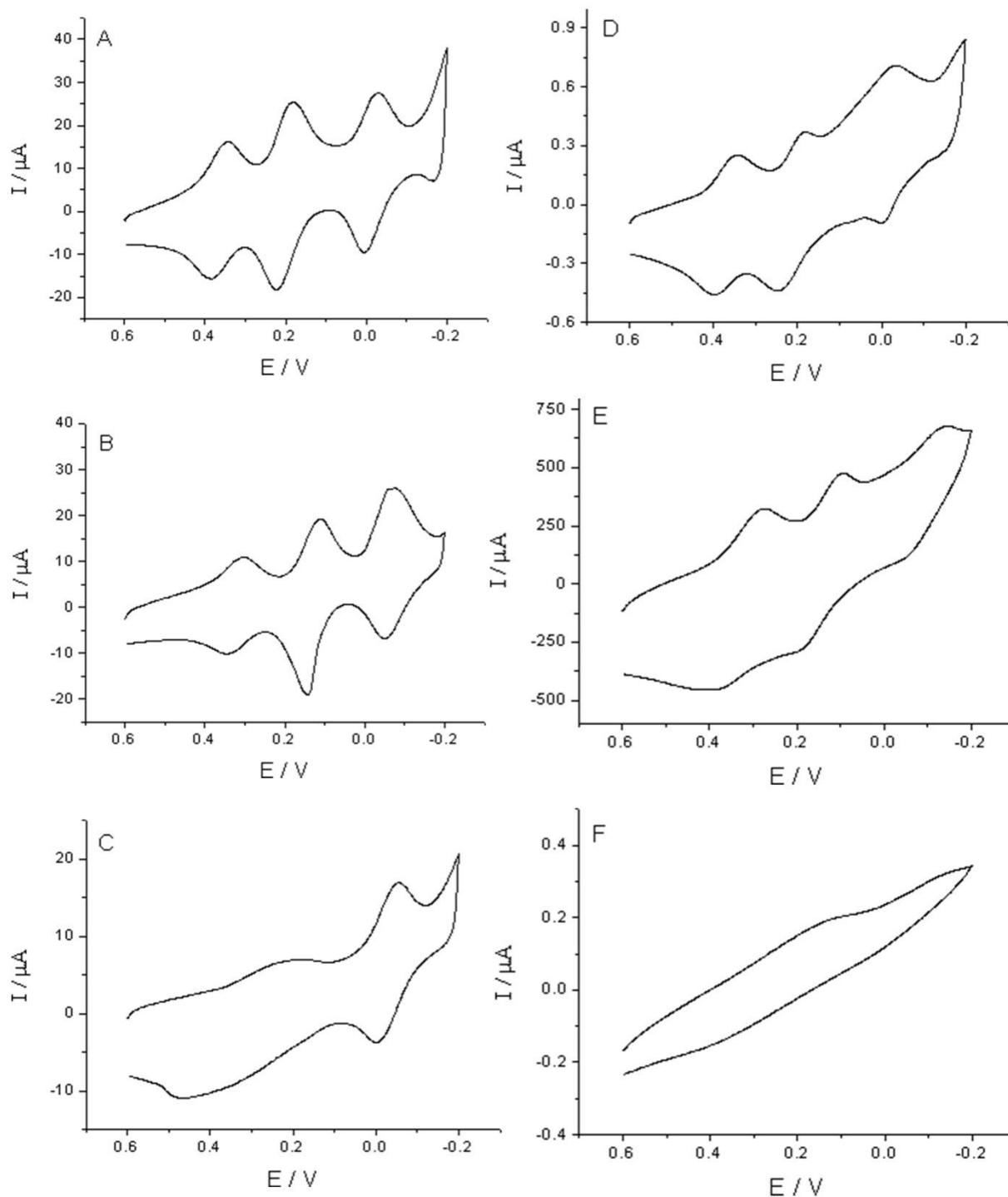
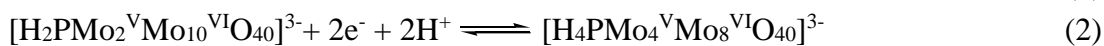


**Figure 3.** The cyclic voltammograms of the  $\text{PMo}_{12}\text{-PAMAM/Au}$  electrode and the  $\text{PMo}_{12}\text{/graphite}$  electrode in 0.5 M  $\text{H}_2\text{SO}_4$  solution (A and D), in pH 2.0 KCl-HCl solution (B and E) and in pH 4.0 citrate solution (C and F), scan rate:  $100 \text{ mVs}^{-1}$ .

Fig. 3A shows the cyclic voltammogram at the  $\text{PMo}_{12}\text{-PAMAM/Au}$  electrode in 0.5 M  $\text{H}_2\text{SO}_4$  aqueous solution. There exhibited three redox couples with the formal potentials ( $E_f = (E_{pa} + E_{pc})/2$ ) of 0.38 (1), 0.238 (2) and 0.003 (3) V (vs. SCE), respectively, similar to those of  $[\text{PMo}_{12}\text{O}_{40}]^{3-}$  in aqueous

solution (not shown). Both voltammograms are characterized by three equivalent waves with practically identical peak potentials. As is known, three redox peaks (1), (2) and (3) represent three successive two electron processes for the couples of  $[\text{PMo}_{12}\text{O}_{40}]^{3-}$  which can be described as follows:



As expected, no redox peak could be seen at both of the electrodes at pH 7.0. This phenomenon can be explained as the redox process of the  $\text{PMo}_{12}$  on the electrode surface need the participation of protons. In general,  $\text{PMo}_{12}$  shows high electroactivity only in strong acidic solutions (see Fig. 3A and 3D). With the pH increased, the peak current decreased gradually at  $\text{PMo}_{12}$ /graphite. The redox peak became obscure at pH 2.0 (Fig. 3E), and even disappeared at pH 4.0 (Fig. 3F). Similarly, when  $\text{pH} > 2.0$ , the  $\text{PMo}_{12}$ /PPy composite film lost its electroactivity, too [44]. There were only two reduction peaks of  $\text{PMo}_{12}$ , their shapes became ill-defined, and even no redox peaks were observed at pH 3.0. However, the electroactivity of the  $\text{PMo}_{12}$  at  $\text{PMo}_{12}$ -PAMAM/Au electrode has been improved remarkably. The three pairs of redox peak were still existed in the aqueous solution of pH 2.0 (Fig. 3B). And the peak currents did not decrease obviously. What is more, the  $\text{PMo}_{12}$  could also take part in the electrochemical reaction at the surface of the electrode in the aqueous solution of pH 4.0 and showed a couple of redox peak, the third couple (Fig. 3C), which indicated that with the cooperation of PAMAM, the localized concentration of  $\text{H}^+$  at the surface of the electrode become higher. This phenomenon can be rationalized as a consequence of the dendrimer protonated state that, by virtue of the  $\text{pK}_a$  of the peripheral functional group of PAMAM ( $-\text{NH}_3^+/-\text{NH}_2$ ,  $\text{pK}_a$  9.52) [45,46] must result in a localized low pH value at the electrode-electrolyte interface.

As is known that the electrocatalysis of the  $\text{PMo}_{12}$  mainly occurred at the third pair of electron transfer reaction, which make it possible to use  $\text{PMo}_{12}$  in electrocatalytic system at pH 4.0. In order to illustrate the electrocatalytic activity in weak acidic media, the  $\text{PMo}_{12}$ -PAMAM host-guest complex membrane has been used for electrocatalytic reduction of  $\text{H}_2\text{O}_2$  and  $\text{S}_2\text{O}_8^{2-}$  in pH 4.0 solution.

### 3.3 The electrochemical reduction of $\text{H}_2\text{O}_2$ and $\text{S}_2\text{O}_8^{2-}$ at the modified electrode.

Fig. 4A shows the cyclic voltammograms of phosphomolybdate-PAMAM complex membrane in pH 4.0 aqueous buffer solution in the absence and presence of  $\text{H}_2\text{O}_2$ . The cathodic peak current at the potential of -0.06 V increased while the anodic peak current decreased as the concentration of  $\text{H}_2\text{O}_2$  increased. As we know, at this potential it is hard to reduce the  $\text{H}_2\text{O}_2$  at bare Au electrode. The reduction peak current was gradually increased with increasing of the  $\text{H}_2\text{O}_2$  concentration, which indicates that the active form of the catalyst takes part in electrochemical reduction of  $\text{H}_2\text{O}_2$ . On the other word, the  $\text{PMo}_{12}$  in the complex film hold its electrocatalytic activity and can be used to catalyze the reduction of  $\text{H}_2\text{O}_2$  at pH 4.0. The catalytic process can be described as follows.

The third pair of electron transfer reaction (Equation (3) above), *i. e.*,



The catalytic reduction reaction of  $\text{H}_2\text{O}_2$  is



As can be seen from Fig. 4A that oxidation peak current was gradually decreased with increasing of the  $\text{H}_2\text{O}_2$  concentration because the reductive product  $[\text{H}_6\text{PMo}_6^{\text{V}}\text{Mo}_6^{\text{VI}}\text{O}_{40}]^{3-}$  was consumed by  $\text{H}_2\text{O}_2$  through the catalytic reduction reaction (Equation (5)).

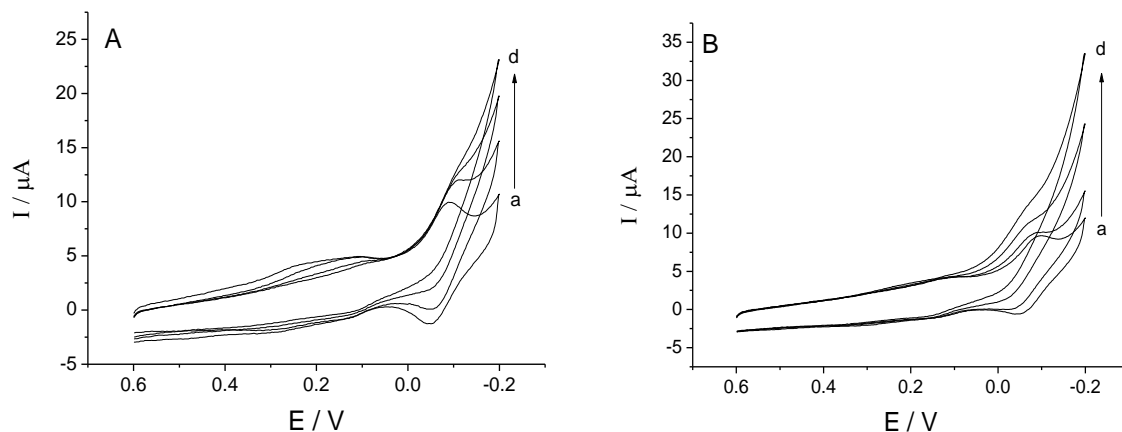
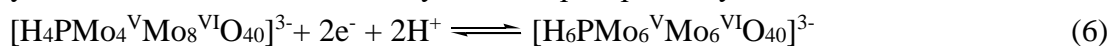


**Figure 4.** Cyclic voltammograms of the  $\text{PMo}_{12}$ -PAMAM/Au electrode in 0.2 M citrate solution (pH 4.0). (A)  $[\text{H}_2\text{O}_2] = 0.0$  mM (a), 1.0 mM (b), 2.0 mM (c), and 3.0 mM (d), and (B)  $[\text{S}_2\text{O}_8^{2-}] = 0.0$  mM (a), 1.0 mM (b), 3.0 mM (c), and 5.0 mM (d). Scan rate is  $100\text{mV s}^{-1}$ .

Fig. 4B gives the cyclic voltammograms of phosphomolybdate-PAMAM complex membrane in pH 4.0 buffer solution in the absence and presence of  $\text{S}_2\text{O}_8^{2-}$ . Similar to  $\text{H}_2\text{O}_2$ , the reduction peak current was creasingly increased with increasing of the  $\text{S}_2\text{O}_8^{2-}$  concentration, and the oxidation peak current was gradually decreased. So, the electrocatalysis of the phosphomolybdate to  $\text{S}_2\text{O}_8^{2-}$  is also similar to  $\text{H}_2\text{O}_2$ .



The catalytic reduction reaction of  $\text{S}_2\text{O}_8^{2-}$  is



It is clear that the  $\text{PMo}_{12}$ -PAMAM nanocomposite film is stable and electroactive in aqueous solutions of pH 4.0. However, as we know, the phosphomolybdate acid is an unstable substances which could be decomposed when the pH of solution is more than 2. Herein, the stability of  $\text{PMo}_{12}$  was improved by a protonated environment which is provided by PAMAM dendrimer.

#### 4. CONCLUSION

The phosphomolybdate-PAMAM nanocomposite film modified gold electrode was successfully fabricated based on the formation of peptide bond between 3-MPA and PAMAM, and the capsulation of dendrimers. The  $\text{PMo}_{12}$  nanoparticles can be located within the dendritic structure of the surface attached PAMAM dendrimers, which is proved by XPS, AFM and CV analysis. Due to the existence of redox centers provided by  $\text{PMo}_{12}$ , the composite film has been used for electrocatalytic reduction of  $\text{H}_2\text{O}_2$  and  $\text{S}_2\text{O}_8^{2-}$  in the aqueous solution of pH 4.0. It is revealed that the electroactivity of  $\text{PMo}_{12}$  is remarkably enhanced in the weak acidic solution under the protonated microenvironment provided by the PAMAM dendrimers, so that the PAMAM encapsulated phosphomolybdate is hopeful to be used as a catalyst in weak acidic media.

## ACKNOWLEDGEMENT

This work was financially supported by the Key University Science Research Project of Anhui Province (KJ2018ZD063), National High Technology Research and Development Program of China (863 program, No. 2013AA065601).

## References

1. S.J. Dong and B.X. Wang, *Electrochim. Acta*, 37(1992)11.
2. B.V.S. Reddy, G. Narasimhulu, P.S. Lakshumma, Y.V. Reddy and J.S. Yadav, *Tetrahedron Lett.*, 53(2012)1776.
3. J.S. Yadav, M. Satyanarayana, E. Balanarsaiah and S. Raghavendra, *Tetrahedron Lett.*, 47(2006)6095.
4. B. Wang, J. Zhang, X. Zou, H.G. Dong and P.P. Yao, *Chem. Eng. J.*, 260(2015)172.
5. X.J. Song, W.C. Zhu, Y. Yan, H.C. Gao, W.X. Gao, W.X. Zhang and M.J. Jia, *J. Mol. Catal. A: Chem.*, 413 (2016)32.
6. S.M. Kendell, T.C. Brown and R.C. Burns, *Catal. Today*, 131(2008)526.
7. Y.Z. Gao, J.A. Syed, H.B. Lu and X.K. Meng, *Appl. Surf. Sci. A*, 360(2016)389.
8. L. Adamczyk and P.J. Kulesza, *Electrochim. Acta*, 56(2011)3649.
9. C. Zea, R. Barranco-Garcia, J. Alcantara, B. Chico, M. Morcillo and, D. de la Fuente, *J. Coatings Techn. Res.*, 14(2017)869
10. A. Manivel, A.M. Asiri, K.A. Alamry, T. Lana-Villarreal and S. Anandan, *Bull. Mater.*, 37(2014)861.
11. D.P. Dubal, B. Ballesteros, A.A. Mohite and P. Gomez-Romero, *ChemSusChem*, 10(2017)731
12. L. Adamczyk, *J. Solid State Electrochem.*, 21(2017)211
13. M.J. Martínez-Morlanes, A.M. Martos, A. Várez and B.J. Levenfeld, *Membr. Sci.*, 492(2015)371.
14. P. Gómez-Romero, J.A. Asensio and S. Borrós, *Electrochim. Acta*, 50(2005)4715.
15. J. Sauk, J. Byun and H. Kim, *J. Power Sources*, 143(2005)136.
16. X. Guo, D.J. Guo, J.S. Wang, X.P. Qiu, L.Q. Chen and W.T. Zhu, *J. Electroanal. Chem.*, 638(2010)167.
17. M.Y. Zhu, X.L. Gao, G.Q. Luo and B. Dai, *J. Power Sources*, 225(2013)27.
18. X.L. Jin, B. He, J.G. Miao, J.H. Yuan, Q.X. Zhang and L. Niu, *Carbon*, 50(2012)3083.
19. L.F. Fan, X.X. Tian, S.M. Shuang and C. Dong, *Chin. J. Chem.*, 34(2016)1177.
20. Z.Y. Bai, C.L. Zhou, N. Gao, H.J. Pang and H.Y. Ma, *RSC Advances*, 6(2016)937.
21. L. Ding, Y.P. Liu, S.X. Guo, J.P. Zhai, A.M. Bond and J. Zhang, *J. Electroanal. Chem.*, 727(2014)69.
22. A. Manivel, R. Sivakumar, S. Anandan and M. Ashokkumar, *Electrocatal.*, 3(2012)22.
23. C.Y. Chen, Y.H. Song and L. Wang, *Electroanal.*, 20(2008)2543.
24. H.X. Guo, Y.Q. Li, L.F. Fan, X.Q. Wu and M.D. Guo, *Electrochim. Acta*, 51(2006)6230.
25. X.L. Wang, H. Zhang, E.B. Wang, Z.B. Han and C.W. Hu, *Mater. Lett.*, 58(2004)1661.
26. A. Antonello, C. Benedetti, F.F. Prez-Pla, M. Kokkionpoulou, K. Kirchhoff, V. Fischer, K. landfester, S. Gross and R. Munoz-Espi, *ACS Applied Mater. Interfaces*, 10(2018)23174
27. X.X. Wang, J.J. Wang, Z.K. Geng, Z. Qian and Z.G. Han, *Dalton Transactions*, 46(2017)7917
28. M. Nunes, D.M. Fernandes, I.M. Rocha, M.F.R. Pereira, I.M. Mbonekalle, P. de Oliveira and C. Freire, *ChemSelect*, 1(2016)6257.
29. D.M. Fernandes and C. Freire, *ChemElectrochem*, 2(2015)269.
30. L. Wang, L. Yue, F. Shi, J.B. Guo, J.L. Yang, J. Lian, X. Luo and Y.K. Guo, *Water Sci. Technol.*, 71(2015)848.
31. D.M. Fernandes, J.G. Vos and C. Freire, *J. Colloid Interface Sci.*, 420(2014)127.
32. A. Manivel and S. Anandan, *J. Solid State Electrochem.*, 15(2011)153.
33. M. Skunik and P.J. Kulesza, *Anal. Chim. Acta*, 631(2009)153.

34. S.M. Chen and Y.H. Fa, *Electroanal.*, 17(2005)579.
35. D. Tomalia and J.M.J. Frechet (Eds.), *Dendrimers and Other Dendritic Polymers*, Wiley–VCH, New York, 2002.
36. D. Astruc and F. Chardac, *Chem. Rev.*, 101(2001)2991.
37. E. Bustos, J. Manriquez, G. Orozco and L.A. Godinez, *Langmuir*, 21(2005)3013.
38. S. Wu, T. Wang, C. Wang, Z. Gao and C. Wang, *Electroanal.*, 19(2007)659.
39. L. Cheng and J.A. Cox, *Electrochem. Commun.*, 3(2001)285.
40. L. Cheng, G.E. Pacey and J.A. Cox, *Electrochim. Acta*, 46(2001)4223.
41. J. Manriquez, E. Juaristi, O. Munoz-Muniz and L.A. Godinez, *Langmuir*, 19(2003)7315.
42. G. Zhang, T. He, Y. Ma, Z. Chen, W. Yang and J. Yao, *Phys. Chem. Chem. Phys.*, 5(2003)2751.
43. Y. Feng, Z. Han, J. Peng, J. Lu, B. Xue, L. Li, H. Ma and E. Wang, *Mater. Lett.*, 60(2006)1588.
44. M. D. Guo and H.X. Guo, *J. Electroanal. Chem.*, 585(2005)28.
45. Y. Lan, E.B. Wang, Y.H. Song, Z.H. Kang, L. Xu, Z. Li and M.Y. Li. *New J. Chem.*, 29(2005)1249.
46. H. Tokuhisa, M. Zhao, L.A. Baker, V.T. Phan, D.L. Dermody, M.E. Garcia, R.F. Pez and R.M. Crooks, T.M. Mayer, *J. Am. Chem. Soc.*, 120(1998)4492.

© 2019 The Authors. Published by ESG ([www.electrochemsci.org](http://www.electrochemsci.org)). This article is an open access article distributed under the terms and conditions of the Creative Commons Attribution license (<http://creativecommons.org/licenses/by/4.0/>).